

Modeling the flare in NGC 1097 from 1991 to 2004 as a tidal disruption event

Xue-Guang Zhang¹★

¹ School of Physical Science and Technology, GuangXi University, No. 100, Daxue Road, 530004, Nanning, P. R. China

20 September 2022

ABSTRACT

In the Letter, interesting evidence is reported to support a central tidal disruption event (TDE) in the known AGN NGC 1097. Considering the motivations of TDE as one probable origination of emission materials of double-peaked broad emission lines and also as one probable explanation to changing-look AGN, it is interesting to check whether are there clues to support a TDE in NGC 1097, not only a changing-look AGN but also an AGN with double-peaked broad emission lines. Under the assumption that the onset of broad H α emission was due to a TDE, the 13years-long (1991-2004) variability of double-peaked broad H α line flux in NGC 1097 can be well predicted by theoretical TDE model, with a $(1 - 1.5)M_{\odot}$ main-sequence star tidally disrupted by the central BH with TDE model determined mass about $(5 - 8) \times 10^7 M_{\odot}$. The results provide interesting evidence to not only support TDE-related origin of double-peaked broad line emission materials but also support TDE as an accepted physical explanation to physical properties of changing-look AGN.

Key words: galaxies:active - galaxies:nuclei - quasars:emission lines - galaxies:Seyfert - transients: tidal disruption events - quasars: individual (NGC 1097)

1 INTRODUCTION

TDEs (Tidal Disruption Events) have been well studied in detail for more than four decades (Rees 1988; Loeb & Ulmer 1997; Cenko et al. 2012; Gezari et al. 2012; Guillochon & Ramirez-Ruiz 2013; Guillochon et al. 2014; Komossa 2015; Wang et al. 2018; Thorp et al. 2019), with accreting fallback debris from stars tidally disrupted by central black holes (BHs) leading to apparent time-dependent variability. Based on TDE expected variability properties, there are more than 100 TDE candidates detected and reported in the literature (see the collected TDE candidates listed in <https://tde.space/>), strongly supporting the idea that TDEs can be used to locate massive BHs and accreting BH systems. More recent reviews on theoretical simulations on TDEs can be found in Stone et al. (2018) and on detected TDE candidates can be found in Gezari (2021). More recent large samples of dozens of TDE candidates can be found in the van Velzen et al. (2021) from the First Half of ZTF (Zwicky Transient Facility) Survey observations and in Sazonov et al. (2021) from the SRG all-sky survey observations.

Along with studying on TDEs, some special spectroscopic features have been considered to be tightly related to TDEs, such as double-peaked broad emission lines, see the discussions in Eracleous et al. (1995) for AGN with double-peaked broad emission lines (hereafter, double-peaked AGN). More detailed discussions on variability properties of double-peaked broad emission lines in TDE candidates can be found in SDSS J0159 in Merloni et al. (2015); Zhang (2021), in ASASSN-14li in Holoien et al. (2016), in PTF09djl in Liu et al. (2017), in PS18kh in Holoien et al. (2019), in AT2018hyz

in Short et al. (2020); Hung et al. (2020), etc.. Therefore, it is interesting to check whether are there double-peaked AGN as host galaxies of TDE candidates. Moreover, TDEs could be probably related to or probably detected in changing-look AGN (AGN with type transitioned between Type 1 and Type 2), such as the detailed results in the changing-look AGN SDSS J0159 in Merloni et al. (2015); LaMassa et al. (2015) and more detailed discussions on a sample of changing-look AGN in Yang et al. (2018) and in the bluest changing-look quasar in Zhang (2021b). Therefore, TDE candidates could be more preferred in changing-look double-peaked AGN.

Fortunately, there is an AGN, the low luminosity AGN NGC 1097, which has been classified as a double-peaked AGN and also as a changing-look AGN. Changing-look properties of NGC 1097 can be confirmed by the following spectroscopic features: no broad emission lines before 1990 as reported in Walsh et al. (1986) but apparently double-peaked broad emission lines in the 1990s and in early 2000s as discussed in Storchi-Bergmann et al. (1993, 2003). Moreover, Kondo et al. (2012) have studied properties of central regions of NGC 1097 through near-infrared spectrum and reported that there are no any evidence for nuclear activity in NGC 1097 in Jul. 18th, 2008, which can be well applied to discuss physical models of flare in NGC 1097. And, the apparently detected double-peaked broad H α lead NGC 1097 to be clearly classified as a double-peaked AGN, although NGC 1097 has central continuum luminosity at 5100Å around 10^{40} erg/s (see Fig. 3 in Storchi-Bergmann et al. (2005)) much lower than common values around 10^{44} erg/s of broad line AGN (Shen et al. 2011).

In the Letter, variability properties of NGC 1097 are well studied to check whether is there strong evidence to support a central TDE in NGC 1097. Section 2 presents our main results on variability of broad H α line flux from 1991 to 2004, and necessary discussions.

★ Corresponding author Email: aexueguang@qq.com

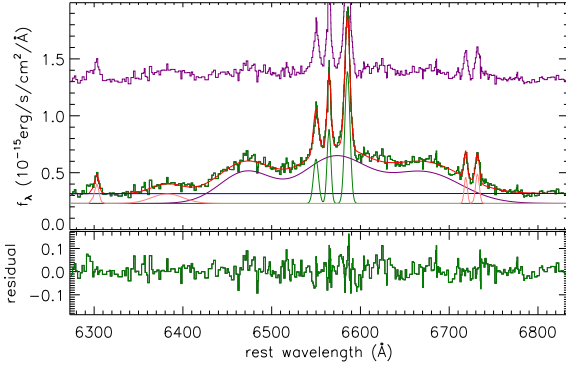


Figure 1. The best fitting results (top panel) and the corresponding residuals (bottom panel) (spectrum minus the best fitting results) to the emission lines around $H\alpha$ of NGC 1097 observed in 2004 by multiple Gaussian functions. In top panel, solid lines in dark green and in red represent the observed spectrum and the corresponding best fitting results, solid lines in purple, blue, pink and dark green show the determined broad $H\alpha$, the determined power law component, the determined [O I] and [S II] doublets, the determined narrow $H\alpha$ and [N II] doublet, respectively. In top panel, solid line in purple represents the expected spectrum plus 1 in 2008 through the spectrum in 2004 with the broad component weakened by TDE model predicted factor of 3.5.

Section 3 gives our final conclusions. And in the Letter, we have adopted the cosmological parameters of $H_0 = 70 \text{ km} \cdot \text{s}^{-1} \text{ Mpc}^{-1}$, $\Omega_\Lambda = 0.7$ and $\Omega_m = 0.3$.

2 LONG-TERM VARIABILITY OF DOUBLE-PEAKED BROAD $H\alpha$ LINE FLUX FROM 1991 TO 2004

Besides spectroscopic results in Storchi-Bergmann et al. (2003) from 1991 to 2001, another spectroscopic results can be collected from the HST (Hubble Space Telescope) mission (ID:8684, PI: Dr. Eracleous) in 2004 with broad $H\alpha$ line flux about $F_{b,obs} \sim (85.6 \pm 7.1) \times 10^{-15} \text{ erg/s/cm}^2$. Here, three broad Gaussian components are applied to describe the broad $H\alpha$ and the other seven narrow Gaussian components are applied to describe the narrow $H\alpha$, [O I] λ 6300, 6363Å, [N II] λ 6548, 6583Å and [S II] λ 6716, 6731Å doublets. Through the Levenberg-Marquardt least-squares minimization technique, the emission components can be well determined and shown in Fig. 1.

As discussed in Storchi-Bergmann et al. (2003), in order to correct effects of aperture sizes on optical spectra with different instruments, total line intensity of narrow $H\alpha$, [N II] and [S II] doublets are applied to determine a scaling factor. Here, the determined total narrow line flux in 2004 is $172 \times 10^{-15} \text{ erg/s/cm}^2$. Meanwhile, the total narrow line flux in Nov. 1991 is $93 \times 10^{-15} \text{ erg/s/cm}^2$ as shown in Storchi-Bergmann et al. (1993). Therefore, the scaling factor for the spectrum in 2004 is about $(93 \times 1.12)/172 \sim 0.61$ with 1.12 as the determined scaling factor for the spectrum in Nov. 1991 relative to the spectrum in Jan. 1996 (the standard spectrum in Storchi-Bergmann et al. (2003)). After corrections of aperture effects, the finally accepted broad $H\alpha$ line flux in 2004 is $\sim 0.61 \times F_{b,obs} = (51.8 \pm 4.3) \times 10^{-15} \text{ erg/s/cm}^2$. Moreover, as shown in Fig. 1, there is a broad component around [O I] λ 6363Å. It is not clear the broad component (line flux about $(3.7 \pm 0.5) \times 10^{-15} \text{ erg/s/cm}^2$) is from the [O I] or from the broad $H\alpha$, however, the lower line flux of the broad component has few effects on the following results. Therefore, there are no further discussions on the weak broad component around [O I] λ 6363Å.

The broad $H\alpha$ line flux in Storchi-Bergmann et al. (2003) and

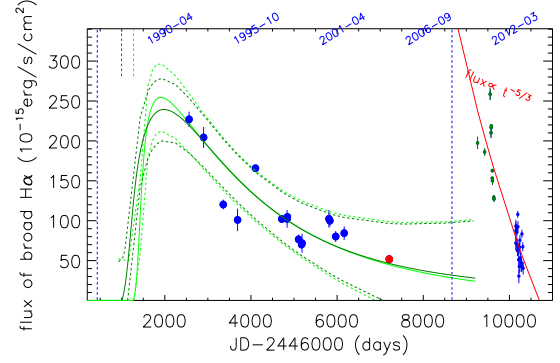


Figure 2. Best descriptions to the variability of broad $H\alpha$ line flux by the TDE model. Large solid blue circles plus error bars are the data points reported in Storchi-Bergmann et al. (2003), large solid red circle plus error bar represents the calculated value in 2004 in the Letter. Solid and dashed lines in green and in dark green represent the best descriptions determined by the TDE model with $\gamma = 4/3$ and with $\gamma = 5/3$ to the variability from 1991 to 2004, and the corresponding 90% confidence bands through the F-test technique, respectively. Small circles plus error bars in dark green and in blue represent the data points collected from Schimoia et al. (2012) and from Schimoia et al. (2015), respectively. Solid red line shows the $t^{-5/3}$ variability trend which can be applied to roughly describe the variability from 2010 to 2013. In the panel, the two vertical blue lines from left to right mark the positions relative to Jan. 1st, 1986 (corresponding to no broad $H\alpha$) and Jul. 18th, 2008 (no apparent central activity through properties of near-infrared spectrum). In top region, the corresponding date information of year-month are marked for the JD-2446000=2000, 4000, 6000, 8000, 10000, respectively, and vertical dashed lines in green and in dark green mark the starting time for the TDE with $\gamma = 4/3$ and $\gamma = 5/3$, respectively.

the new calculated broad $H\alpha$ line flux in 2004 can lead to the long-term variability over ten years from 1991 to 2004 shown in Fig. 2. It is interesting that the flux variability of broad $H\alpha$ has a systematically time-dependent declined trend, similar as TDE expected properties. Then, the more recent theoretical TDE model well discussed in Guillochon & Ramirez-Ruiz (2013); Guillochon et al. (2014); Mockler et al. (2019) can be applied as follows to check whether a TDE model can be applied to describe the long-term variability of broad $H\alpha$ flux.

There are public codes on the theoretical TDE model, such as the TDEFIT and the MOSFIT. Here, based on the more recent discussions in Mockler et al. (2019), the theoretical TDE model can be applied by the following four steps to model variability of NGC 1097, similar as what we have done in Zhang (2022) to describe the X-ray variability in the TDE candidate *Swift* J2058.4+0516 with relativistic jet.

First, standard templates of viscous-delayed accretion rates \dot{M}_{at} are created by,

$$\dot{M}_{at} = \frac{\exp(-t/T_v)}{T_v} \int_0^t \exp(t'/T_v) \dot{M}_{f_{bt}} dt' \quad (1)$$

$$\dot{M}_{f_{bt}} = dm/de \times de/dt = dm/de \times \frac{(2\pi G M_{BH})^{2/3}}{3 t^{5/3}}$$

with dm/de as the TDEFIT provided distributions of debris mass dm as a function of specific binding energy e after a star is disrupted, M_{BH} as central BH mass, and $\dot{M}_{f_{bt}}$ as TDEFIT and MOSFIT provided templates of fallback material rates for standard cases with central BH of $M_{BH} = 10^6 M_\odot$ and disrupted main-sequence star of $M_* = 1 M_\odot$ and with a grid of the listed impact parameters β_{temp} in Guillochon & Ramirez-Ruiz (2013), and T_v as the vis-

cous time after considering the viscous delay effects as discussed in [Guillochon & Ramirez-Ruiz \(2013\)](#); [Mockler et al. \(2019\)](#). Here, a grid of 31 $\log(T_{v,temp}/\text{years})$ range from -3 to 0 are applied to create templates of \dot{M}_{at} for each impact parameter. Finally, templates of \dot{M}_{at} include 736 (640) time-dependent viscous-delayed accretion rates for 31 different T_v of each 23 (20) impact parameters for the main-sequence star with polytropic index γ of 4/3 (5/3).

Second, simple linear interpolations are applied to determine accretion rates $\dot{M}_a(T_v, \beta)$ for TDEs with input model parameters of β and T_v different from the list values in β_{temp} and in $T_{v,temp}$. Assuming that β_1, β_2 in the β_{temp} are the two values nearer to the input β and T_{v1}, T_{v2} in the $T_{v,temp}$ are the two values nearer to the input T_v , the expected $\dot{M}_a(T_v, \beta)$ can be estimated by

$$\begin{aligned} \dot{M}_a(T_v, \beta_1) &= \dot{M}_{at}(T_{v1}, \beta_1) + \\ &\quad \frac{T_v - T_{v1}}{T_{v2} - T_{v1}} (\dot{M}_{at}(T_{v2}, \beta_1) - \dot{M}_{at}(T_{v1}, \beta_1)) \\ \dot{M}_a(T_v, \beta_2) &= \dot{M}_{at}(T_{v1}, \beta_2) + \\ &\quad \frac{T_v - T_{v1}}{T_{v2} - T_{v1}} (\dot{M}_{at}(T_{v2}, \beta_2) - \dot{M}_{at}(T_{v1}, \beta_2)) \\ \dot{M}_a(T_v, \beta) &= \dot{M}_a(T_v, \beta_1) + \frac{\beta - \beta_1}{\beta_2 - \beta_1} (\dot{M}_a(T_v, \beta_2) - \dot{M}_a(T_v, \beta_1)) \end{aligned} \quad (2)$$

Third, for TDEs with input M_{BH} and M_* different from $10^6 M_\odot$ and $1 M_\odot$, as discussed in [Guillochon & Ramirez-Ruiz \(2013\)](#); [Mockler et al. \(2019\)](#), actual viscous-delayed accretion rates \dot{M} and the corresponding time information are created by the following scaling ratios applied with input BH mass, mass and radius of the disrupted main-sequence star,

$$\begin{aligned} \dot{M} &= M_{BH,6}^{-0.5} \times M_*^2 \times R_*^{-1.5} \times \dot{M}_a(T_v, \beta) \\ t &= (1+z) \times M_{BH,6}^{0.5} \times M_*^{-1} \times R_*^{1.5} \times t_a(T_v, \beta) \end{aligned} \quad (3)$$

, where $M_{BH,6}$, M_* , R_* and z represent central BH mass in unit of $10^6 M_\odot$, stellar mass in unit of M_\odot , stellar radius in unit of R_\odot and redshift of host galaxy of a TDE, respectively. And the mass-radius relation discussed in [Tout \(1996\)](#) has been accepted in the Letter for main-sequence stars.

Fourth, the time-dependent output emission spectrum in rest frame based on the TDE model expected accretion rate $\dot{M}(t)$ can be determined by the simple black-body photosphere model as discussed in [Guillochon et al. \(2014\)](#); [Mockler et al. \(2019\)](#),

$$\begin{aligned} F_\lambda(t) &= \frac{2\pi G c^2}{\lambda^5} \frac{1}{\exp(hc/(k\lambda T_p(t))) - 1} \left(\frac{R_p(t)}{D}\right)^2 \\ R_p(t) &= R_0 \times a_p \left(\frac{\eta \dot{M}(t) c^2}{1.3 \times 10^{38} M_{BH}/M_\odot}\right)^{1/p} \\ T_p(t) &= \left(\frac{\eta \dot{M}(t) c^2}{4\pi \sigma_{SB} R_p^2}\right)^{1/4} \quad a_p = (GM_{BH} \times \left(\frac{t_p}{\pi}\right)^2)^{1/3} \end{aligned} \quad (4)$$

where D means the distance to the earth calculated by redshift $z = 0.00424$ (the redshift of NGC 1097), k is the Boltzmann constant, $T_p(t)$ and $R_p(t)$ represent the time-dependent effective temperature and radius of the photosphere, respectively, and η is the energy transfer efficiency smaller than 0.4, σ_{SB} is the Stefan-Boltzmann constant, and t_p is the time information of the peak accretion. Then, based on the $F_{5100\text{\AA}}(t)$ in rest frame, time-dependent broad $H\alpha$ line fluxes $f_{H\alpha}(t)$ can be determined by

$$f_{H\alpha}(t) = F_{5100\text{\AA}}(t) \times K_{cl} \quad (5)$$

with K_{cl} as the intensity ratio of broad $H\alpha$ line flux to continuum

Table 1. Parameters of TDE models for NGC 1097

parameter	prior	p0	value ^a	value ^b
$\log(M_{BH,6})$	[-3, 3]	1.	1.86 ± 0.22	1.73 ± 0.34
$\log(M_*/M_\odot)$	[-2, 1.7]	0.	0.16 ± 0.17	0.12 ± 0.13
$\log(\beta)(4/3)$	[-0.22, 0.6]	0.	0.12 ± 0.09	...
$\log(\beta)(5/3)$	[-0.3, 0.4]	0.	...	-0.06 ± 0.06
$\log(T_{vis})$	[-3, 0]	-1.	-0.14 ± 0.12	-0.17 ± 0.14
$\log(\eta)$	[-3, -0.4]	-1.	-2.28 ± 0.75	-2.69 ± 0.76
$\log(R_0)$	[-3, 3]	1.	0.13 ± 0.55	-0.10 ± 0.55
$\log(l_p)$	[-3, 0.6]	0.	-0.16 ± 0.12	-0.19 ± 0.12
$\log(K_{cl})$	[-3, 6]	1.	1.55 ± 0.59	1.65 ± 0.64

Notes: The first column shows the applied model parameters. The second column shows limitations of the prior uniform distribution of each model parameter. The third column with title "p0" lists starting value of each parameter. The fourth column with column title marked with ^a means the values of model parameters for the TDE model with $\gamma = 4/3$. The fifth column with column title marked with ^b means the values of model parameters for the TDE model with $\gamma = 5/3$.

emission intensity at 5100\AA in rest frame, through the strong correlation between continuum luminosity and broad $H\alpha$ line luminosity ([Greene & Ho 2005](#); [Zhang et al. 2008](#)).

When the procedure above is applied to describe the observed variability of broad $H\alpha$ line flux, there is only one limitation that the determined tidal disruption radius $R_{TDE} \propto (M_*)^{-1/3} (M_{BH})^{-2/3} R_*$ to be larger than event horizon of central BH $R_G = 2GM_{BH}/c^2$.

Finally, the theoretical TDE model expected time dependent light curves $f_{H\alpha}(t)$ can be described by eight model parameters, central BH mass $\log(M_{BH})$, stellar mass $\log(M_*)$ (corresponding stellar radius R_* calculated by the mass-radius relation), energy transfer efficiency $\log(\eta)$, impact parameter $\log(\beta)$, viscous timescale $\log(T_v)$, parameters l_p and R_0 related to the black-body photosphere model, and ratio K_{cl} . Then, through the well-known maximum likelihood method combining with the Markov Chain Monte Carlo (MCMC) technique ([Foreman-Mackey et al. 2013](#)), the variability of broad $H\alpha$ line fluxes in NGC 1097 can be well predicted and shown in Fig. 2 from 1991 to 2004, accepted prior uniform distributions of the model parameters and the corresponding starting values listed in Table 1. Two-dimensional posterior distributions of the model parameters are shown in Fig. 3. And the final accepted model parameters and corresponding uncertainties are also listed in Table 1. Here, the uncertainty of each parameter is determined by the half width at half maximum of distribution of each parameter. Based on the determined model parameters, the expected TDE is starting from $\text{JD}=2447275 \pm 140$ (around Apr. 24th, 1988) and from $\text{JD}=2446997 \pm 180$ (around Jul. 20th, 1988) for the model with $\gamma = 4/3$ and $\gamma = 5/3$, respectively. If considering the mass limitation of central disrupted stellar in [Guillochon & Ramirez-Ruiz \(2013\)](#); [Mockler et al. \(2019\)](#): $M_* < 0.3M_\odot$ or $M_* > 22M_\odot$ for $\gamma = 5/3$, the TDE model with $\gamma = 4/3$ is preferred in NGC 1097. The determined model parameters have reasonable values, compared with the values for the other optical TDEs candidates in the literature, providing direct and interesting clues to support a central TDE in NGC 1097 from 1991 to 20004.

Then, it is interesting to check whether the TDE model predicted $H\alpha$ line flux is lower enough to be consistent with the reported none apparent AGN activity in 2008 in [Kondo et al. \(2012\)](#). As shown in Fig. 2, the expected broad $H\alpha$ line flux in 2008 is about $25 \times 10^{-15} \text{erg/s/cm}^2$, about 3.5 times weaker than that observed in 2004. Now, it is interesting to check whether so weak broad $H\alpha$ component

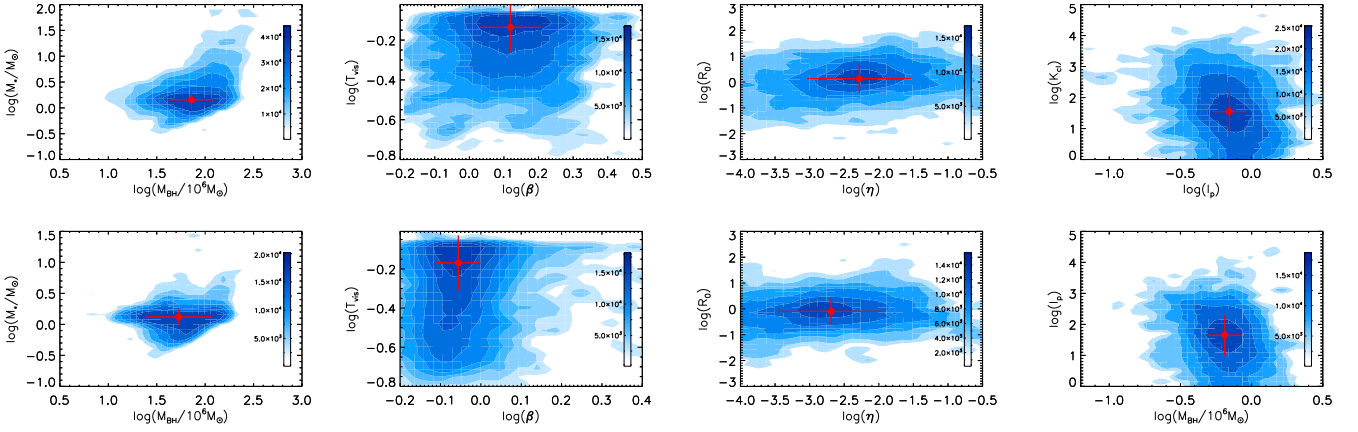


Figure 3. Two-dimensional posterior distributions of the model parameters with $\gamma = 4/3$ (top panels) and with $\gamma = 5/3$ (bottom panels). In each panel, solid red circle plus error bars show the final accepted values and corresponding uncertainties of the model parameters. Contour levels with different colors represent different number densities, as shown in the color bar in each panel.

can be well detected in spectrum. As an oversimplified example, based on the observed spectrum in 2004 with the broad component weakened by a factor of 3.5 (similar values for the TDE model with different γ), the expected spectrum in 2008 is shown in Fig. 2: no apparent broad H α , to be consistent with the reported none-activity in NGC 1097 in 2008 in Kondo et al. (2012). In other words, the none apparent activity in 2008 reported in Kondo et al. (2012) could be simply expected, under the assumption of a central TDE in NGC 1097. Therefore, the determined TDE model is reasonable.

Based on the best descriptions shown in Fig. 2, the variability from 1991 to 2004 in NGC 1097 can be well predicted by theoretical TDE model, under the assumption of double-peaked broad H α emissions related to a TDE. However, there is an interesting question whether is there further evidence to support the emission materials of the double-peaked broad emission lines related to the central TDE. As discussed in Storchi-Bergmann et al. (2003), the double-peaked features provide the corresponding emission regions with inner radius about $225R_G$ and outer radius about $800R_G$ (here, R_G is two times of the unit used in Storchi-Bergmann et al. (2003)). If the double-peaked broad H α were related to the central TDE, we could expect the regions of accreting debris in the TDE could cover the emission regions for the double-peaked broad H α . Based on the model parameters, the distance of accreting debris as discussed in (Guillochon et al. 2014) can be roughly estimated by $R_o \sim 2 \times (\frac{GM_{BH} \times t^2}{\pi^2})^{1/3}$, leading to $R_o \sim 3200R_G$ in 2000 (where t is about 3400days), indicating the accreting debris totally cover the expected emission regions of the double-peaked broad H α in NGC 1097. Therefore, it is plausible to accept that the double-peaked broad H α are from accreting debris in the central TDE in NGC 1097. Furthermore, through the well measured stellar velocity dispersion about 190km/s in NGC 1097 in Lewis & Eracleous (2006) and discussed in Storchi-Bergmann et al. (2003); Onishi et al. (2015), the central BH mass of NGC 1097 has been reported to be around $10^8 M_\odot$ through the well-known $M_{BH} - \sigma$ (Ferrarese & Merritt 2000; Gebhardt et al. 2000; Kormendy & Ho 2013; Batiste et al. 2017; Bennert et al. 2021), simply consistent with the TDE model determined BH mass after considering the uncertainties, providing further evidence to support the central TDE in NGC 1097.

Before end of the section, three further points are noted. First, besides the long-term variability of double-peaked broad H α over ten

years from 1991 to 2004, there are apparent variability of double-peaked broad H α from 2010 to 2013, as discussed in Schimoia et al. (2012, 2015), which are shown as small circles in Fig. 2. Considering the long-term variability from 1991 to 2013 in NGC 1097 shown in Fig. 2, the variability pattern is quite like the case discussed in Campana et al. (2015); Grupe et al. (2015) in the known changing-look AGN IC 3599. Different models have been proposed to explain the multiple flares. Campana et al. (2015) have shown that a tidal stripping in partial TDE can lead to repeated tidal disruption flares. However, Grupe et al. (2015) have shown that the second flare in IC 3599 should be related to accretion disk variability. Mandel & Levin (2015) have shown that binary stars disrupted by central massive BH (double TDE) can lead to repeated flares. There are so-far no confirmed physical origin of repeated flares in IC 3599, neither in NGC 1097. However, based on special properties of NGC 1097, further discussions can be given on the proposed models. Mandel & Levin (2015) have shown that the majority of double-star disruptions produce two flares close enough in time that they overlap. As NGC 1097 was apparently inactive in 2008 (Kondo et al. 2012), between the two peaks of H α flux, then this scenario in Mandel & Levin (2015) should be disfavoured. Probably, the second flare in NGC 1097 should be related to an independent TDE, because the TDE expected $t^{-5/3}$ (shown as solid red line in Fig. 2) can be roughly applied to describe the variability from 2011 to 2013.

Second, as the discussed variability around 2010 in Schimoia et al. (2012) (time duration less than 400days), there is an interesting plateau phase (shown in Fig. 5 in Schimoia et al. (2012)), which can not be expected by standard TDE model. The interesting variability properties could including effects of accretion disk variability. Therefore, long-term variabilities with scale about ten years could be simply expected by standard TDE model, however, short-term variability with time scale about hundreds of days should be related to central accretion disk variability. Therefore, the long-term variability from 1991 to 2004 is mainly considered in the Letter, due to well predicted by the standard TDE model.

Third, as the shown best fitting results in Fig. 2 from 1991 to 2004, a decay in flux of a factor 5 in 10 years is slow for standard TDEs. However, after considering viscous delay effects, the decaying trend should be quite flatter than $t^{-5/3}$. Similar flat decay can be found in some other reported TDEs, such as the PS1-11af, TDE2, etc.

shown in Fig. 1 in Mockler et al. (2019) with magnitude decay about 1.5-2mags (flux decay factor about 4-6) from the time with peak intensity to late times. Therefore, the slower decay trend in NGC 1097 can be well accepted. Certainly, as reported and discussed in Gezari et al. (2008, 2009) and simple descriptions in Gezari (2021), quite flatter decaying trend could be also found in TDE expected light curves at late stages, such as in the TDE candidate D3-13 with index $t^{-0.82}$ at late stages. Therefore, it is interesting to consider whether the flatter decaying trend in NGC 1097 is due to catching the event in the late stages. If accepted the variability from 1991 to 2004 from TDE expected variability at late stages, expected starting time of the TDE should be earlier than 1986, under simply considering the flatter decaying trend at late stages having similar (or even two times) time duration as the steeper decaying trend at early stages around the peak. However, there are no broad H α emissions in 1986, indicating the consideration of catching the event in the late stages should be not favoured to explain the flatter decaying trend in NGC 1097. Moreover, based on the TDE model determined parameters, the peak accretion rate is estimated to be $\dot{M} \sim 0.02M_{\odot}/\text{year}$, and the total accreted mass during the 13years-long flare is estimated to be $0.2M_{\odot}$. Considering the determined energy efficiency about $\log(\eta) \sim -2.28$, the corresponding observed peak bolometric luminosity is about $\eta \times \dot{M}c^2 \sim 6 \times 10^{42}\text{erg/s}$. However, after considering the probable intrinsic reddening effects with $A_V = 3\text{mag}$ as discussed in Storchi-Bergmann et al. (2005), the intrinsic peak bolometric luminosity is about $9 \times 10^{43}\text{erg/s}$ well consistent with the peak bolometric luminosities around 10^{44}erg/s of the other TDE candidates as discussed in Mockler et al. (2019), to support the central TDE in NGC 1097.

3 CONCLUSIONS

Finally, we give our main conclusions as follows. Under the assumption of double-peaked broad emission lines coming from TDE related debris, theoretical TDE model with a $1 - 1.5M_{\odot}$ main-sequence star disrupted by the central BH with TDE model determined mass about $(5 - 8) \times 10^7 M_{\odot}$ can be well applied to predict the 13years-long (1991-2004) variability of double-peaked broad H α line fluxes in the well-known low luminosity AGN NGC 1097, providing interesting evidence to support a central TDE in NGC 1097 which has been classified as both a changing-look AGN and a double-peaked AGN. Therefore, NGC 1097 is so-far the best candidate to support the TDE related origin of double-peaked broad Balmer emission materials and to support TDE as the physical explanation to properties of changing-look AGN.

ACKNOWLEDGEMENTS

Zhang gratefully acknowledges the anonymous referee for giving us constructive comments and suggestions greatly improving our paper. Zhang gratefully acknowledges the great comments and suggestions from Prof. T. Storchi-Bergmann, and acknowledges the funding support from NSFC-12173020. This letter has made use of the NASA/IPAC Extragalactic Database (NED) operated by the Jet Propulsion Laboratory, Caltech, and the observation data with the NASA/ESA Hubble Space Telescope obtained from the Space Telescope Science Institute, and the public codes of TDE-FIT (<https://github.com/guillochon/tdefit>) and MOSFIT (<https://github.com/guillochon/mosfit>).

DATA AVAILABILITY

The data underlying this article will be shared on request to the corresponding author (aexueguang@qq.com).

REFERENCES

- Batiste, M.; Bentz, M. C.; Raimundo, S. I.; Vestergaard, M.; Onken, C. A., 2017, *ApJL*, 838, 10
- Bennert, V. N.; Treu, T.; Ding, X.; et al., 2021, *ApJ*, 921, 36
- Campana, S.; Mainetti, D.; Colpi, M.; Lodato, G.; D'Avanzo, P.; Evans, P. A.; Moretti, A., 2015, *A&A*, 581, 17
- Cenko, S. B.; Krimm, H. A.; Horesh, A., et al., 2012, *ApJ*, 753, 77
- Eracleous, M.; Livio, M.; Halpern, J. P.; Storchi-Bergmann, T., 1995, *ApJ*, 438, 610
- Ferrarese, F.; Merritt, D., 2000, *ApJL*, 539, 9
- Foreman-Mackey, D.; Hogg, D. W.; Lang, D.; Goodman, J., 2013, *PASP*, 125, 306
- Gebhardt, K., et al., 2000, *ApJL*, 539, 13
- Gezari, S.; Basa, S.; Martin, D. C.; et al., 2008, *ApJ*, 676, 944
- Gezari, S.; Heckman, T.; Cenko, S. B.; et al., 2009, *ApJ*, 698, 1367
- Gezari, S.; Chornock, R.; Rest, A., et al., 2012, *Nature*, 485, 217
- Gezari, S., 2021, *ARA&A*, 59, 21
- Greene, J. E.; & Ho, L. C., 2005, *ApJ*, 630, 122
- Grupe, D.; Komossa, S.; Saxton, R., 2015, *ApJ*, 803, 28
- Guillochon, J.; & Ramirez-Ruiz, E., 2013, *ApJ*, 767, 25
- Guillochon, J.; Manukian, H.; Ramirez-Ruiz, E., 2014, *ApJ*, 783, 23
- Holoien, T. W. S.; Kochanek, C. S.; Prieto, J. L.; et al., 2016, *MNRAS*, 455, 2918
- Holoien, T. W. S.; Huber, M. E.; Shappee, B. J.; et al., 2019, *ApJ*, 880, 120
- Hung, T.; Foley, R. J.; Ramirez-Ruiz, E.; et al., 2020, *ApJ*, 903, 31
- Komossa, S., 2015, *JHEAp*, 7, 148
- Kondo, T.; Kaneda, H.; Oyabu, S., et al., 2012, *ApJL*, 751, 18
- Kormendy, J.; Ho, L. C., 2013, *ARA&A*, 51, 511
- LaMassa, S. M.; Cales, C.; Moran, E. C.; et al., 2015, *ApJ*, 800, 144
- Lewis, K. T.; & Eracleous, M., 2006, *ApJ*, 642, 711
- Liu, F. K.; Zhou, Z. Q.; Cao, R.; Ho, L. C.; Komossa, S., 2017, *MNRAS Letter*, 472, 99
- Loeb, A.; Ulmer, A., 1997, *ApJ*, 489, 573
- Mandel, I.; Levin, Y., 2015, *ApJL*, 505, 4
- Merloni, A.; Dwelly, T.; Salvato, A. G.; et al., 2015, *MNRAS*, 452, 69
- Mockler, B.; Guillochon, J.; Ramirez-Ruiz, E., 2019, *ApJ*, 872, 151
- Onishi, K.; Iguchi, S.; Sheth, K.; Kohno, K., 2015, *ApJ*, 806, 39
- Rees, M. J., 1988, *Nature*, 333, 523
- Sazonov, S.; Gilfanov, M.; Medvedev, P.; et al., 2021, *MNRAS*, 508, 3820
- Schimoia, J. S.; Storchi-Bergmann, T.; Nemmen, R. S.; Winge, C.; Eracleous, M., 2012, *ApJ*, 748, 145
- Schimoia, J. S.; Storchi-Bergmann, T.; Grupe, D., et al., 2015, *ApJ*, 800, 63
- Shen, Y.; Richards, G. T.; Strauss, M. A.; et al., 2011, *ApJS*, 194, 45
- Short, P.; Nicholl, M.; Lawrence, A.; Gomez, S.; et al., 2020, *MNRAS*, 498, 4119
- Stone, N. C.; Kesden, M.; Chang, R. M.; van Velzen, S.; *General Relativity and Gravitation*, 2018, arXiv:1801.10180
- Storchi-Bergmann, T.; Baldwin, J. A.; Wilson, A. S., 1993, *ApJL*, 410, 11
- Storchi-Bergmann, T.; Nemmen, R. S.; Eracleous, M.; et al., 2003, *ApJ*, 489, 8
- Storchi-Bergmann, T.; Nemmen, R. S.; Spinelli, P. F.; Eracleous, M.; Wilson, A. S.; Filippenko, A. V.; Livio, M., 2005, *ApJL*, 624, 13
- Thorp, S.; Chadwick, E.; Sesana, A., 2019, *MNRAS*, 488, 4042
- Tout, C. A.; Pols, O.; Eggleton, P.; Han, Z., 1996, *MNRAS*, 281, 257
- van Velzen, S.; Gezari, S.; Hammerstein, E.; et al., 2021, *ApJ*, 908, 4
- Walsh, J. R.; Nandy, K.; Thompson, G. I.; Meaburn, J., 1986, *MNRAS*, 220, 453
- Wang, T.; Yan, L.; Dou, L., et al., 2018, *MNRAS*, 477, 2943
- Yang, Q.; Wu, X. B.; Fan, X., et al., 2018, *ApJ*, 862, 109
- Zhang, X. G.; Dultzin, D.; Wang, T. G., 2008, *MNRAS*, 385, 1087
- Zhang, X. G., 2021, *MNRAS Letter*, 500, 57

Zhang, X. G., 2021b, ApJ, 919, 13

Zhang, X. G., 2022, ApJ accepted, Arxiv:2202.11265